STRUCTURAL CHEMISTRY

ISSN: 2053-2296
journals.iucr.org/c

Transferred multipolar atom model for 10β,17β-dihydroxy-17α-methylestr-4-en-3-one dihydrate obtained from the biotransformation of methyloestrenolone

Muhammad Umer Faroque, Sammer Yousuf, Salman Zafar, M. Iqbal Choudhary and Maqsood Ahmed

Acta Cryst. (2016). C**72**, 398–404

Acta Cryst C STRUCTURAL CHEMISTRY
ISSN 2053-2296

Transferred multipolar atom model for 10β,17β-dihydroxy-17α-methylestr-4-en-3-one dihydrate obtained from the biotransformation of methyloestrenolone

Muhammad Umer Faroque,[a] Sammer Yousuf,[b]* Salman Zafar,[c] M. Iqbal Choudhary[b] and Maqsood Ahmed[a]*

[a]Department of Chemistry, The Islamia University of Bahawalpur, Bahawalpur 63100, Pakistan, [b]H.E.J. Research Institute of Chemistry, International Center for Chemical and Biological Sciences, University of Karachi, Karachi 75270, Pakistan, and [c]Institute of Chemical Sciences, University of Peshawar, Peshawar 25120, Pakistan. *Correspondence e-mail: dr.sammer.yousuf@gmail.com, maqsood.ahmed@iub.edu.pk

Received 27 February 2016
Accepted 31 March 2016

Edited by F. A. Almeida Paz, University of Aveiro, Portugal

Keywords: steroids; estrane; biotransformation; ELMAM2; crystal structure; methyloestrenolone; estr-4-en-3-one; independent atom model (IAM); transferred multipolar atom model.

CCDC reference: 1471646

Supporting information: this article has supporting information at journals.iucr.org/c

Biotransformation is the structural modification of compounds using enzymes as the catalysts and it plays a key role in the synthesis of pharmaceutically important compounds. 10β,17β-Dihydroxy-17α-methylestr-4-en-3-one dihydrate, $C_{19}H_{28}O_3 \cdot 2H_2O$, was obtained from the fungal biotransformation of methyloestrenolone. The structure was refined using the classical independent atom model (IAM) and a transferred multipolar atom model using the ELMAM2 database. The results from the two refinements have been compared. The ELMAM2 refinement has been found to be superior in terms of the refinement statistics. It has been shown that certain electron-density-derived properties can be calculated on the basis of the transferred parameters for crystals which diffract to ordinary resolution.

1. Introduction

Biotransformation or biocatalysis is the structural modification of compounds using enzymes as the catalysts (Mahato & Garai, 1997). Biotransformation using whole-cell cultures of microorganisms is an efficient method for the production of libraries of structurally diverse molecules, starting from a single substrate (Mahato & Garai, 1997; Ahmad *et al.*, 2014; Khan *et al.*, 2014; Zafar *et al.*, 2012; Leon *et al.*, 1998; Holland, 1999). This methodology has been applied to the synthesis of bioactive molecules of varying nature (Choudhary *et al.*, 2012; Monagas *et al.*, 2010; Liu & Yu, 2010; Cao *et al.*, 2015; Wang, 2015). Biotransformation has found application in organic synthesis as well. Due to the specific nature of enzymes, the reactions take place with high stereo- and regioselectivity (Wang *et al.*, 2000; Wang, 2015; Palomo & Filice, 2015). Therefore, biotransformation plays a key role in the synthesis of pharmaceutically important compounds.

The chemical properties of the molecule depend on the charge–density distribution (Coppens, 1998; Jayatilaka, 2012). A detailed knowledge of the structural parameters, stereochemistry, planarity and the mutual arrangement of the molecule is required to better understand the structure–activity relationships. In addition, knowledge of the intra- and intermolecular interactions is important for the design of new drugs and modelling the interactions with proteins. The commonly used independent atom model (IAM) does not give all the information about the intermolecular interactions and is likely to produce severe systematic errors in the refined atomic

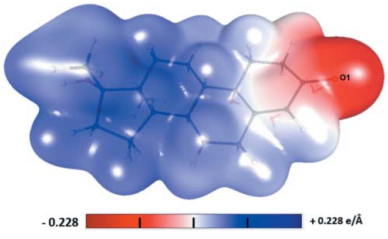

Table 1
Experimental details.

Crystal data	
Chemical formula	$C_{19}H_{28}O_3{\cdot}2H_2O$
M_r	340.44
Crystal system, space group	Orthorhombic, $P2_12_12_1$
Temperature (K)	100
a, b, c (Å)	6.9028 (6), 11.0334 (10), 24.451 (2)
V (Å^3)	1862.2 (3)
Z	4
Radiation type	Mo $K\alpha$
μ (mm^{-1})	0.09
Crystal size (mm)	0.27 × 0.10 × 0.07
Data collection	
Diffractometer	Bruker SMART CCD detector
Absorption correction	Multi-scan (*SADABS*; Bruker, 2000)
T_{min}, T_{max}	0.977, 0.994
No. of measured, independent and observed [$I > 2\sigma(I)$] reflections	13666, 2792, 2792
R_{int}	0.052
(sin $\theta/\lambda)_{max}$ (Å^{-1})	0.667
Refinement	
$R[F^2 > 2\sigma(F^2)]$, $wR(F^2)$, S	0.048, 0.116, 0.95
No. of reflections	2792
No. of parameters	217
H-atom treatment	H-atom parameters constrained
$\Delta\rho_{max}$, $\Delta\rho_{min}$ (e Å^{-3})	0.35, −0.26

Computer programs: *SMART* (Bruker, 2000), *SAINT* (Bruker, 2000), *SIR92* (Altomare *et al.*, 1993), *MoPro* (Jelsch *et al.*, 2005), *Mercury* (Macrae *et al.*, 2006), *MoProViewer* (Guillot, 2011) and *publCIF* (Westrip, 2010).

parameters (Ruysink & Vos, 1974). Experimental electron-density analysis is carried out by X-ray diffraction of mono-crystals at ultra-high resolution (Coppens, 1998). However, the difficult part is the separation of the anisotropic atomic mean-square displacements from the static molecular electron distribution (Hirshfeld, 1976). Proper experimental deconvolution requires diffraction data measured at ultra-high resolution. However, effective thermal displacement deconvolution and meaningful electron-density distributions can be achieved even at lower resolutions by transferring the parameters from an electron-density database (Pichon-Pesme *et al.*, 1995; Jelsch *et al.*, 1998; Dittrich *et al.*, 2004, 2005, 2007; Ahmed *et al.*, 2011). Transferring electron-density parameters is comparable to constraining the atomic coordinates at their most likely values. The transferability of atomic electron densities was tested for the first time by Brock *et al.* (1991) who applied atomic charge–density parameters from an accurate low-temperature study of perylene to diffraction data collected at several temperatures on naphthalene and anthracene crystals.

The ELMAM database (Zarychta *et al.*, 2007) has been extended to ELMAM2 (Domagała *et al.*, 2012) from protein atom types to common organic molecules, and is based on optimal local-coordinate systems (Domagała & Jelsch, 2008). An automatic transfer procedure of the ELMAM2 database is now available in the *MoPro* software (Guillot *et al.*, 2001; Jelsch *et al.*, 2005). Different atom types in a molecule are recognized according to the nature and number of their neighbours. For most atoms, only the first shell of neighbours is analysed, while for H and O atoms, the second and third shells are investigated, respectively (Domagała & Jelsch, 2008; Domagała *et al.*, 2012). Using the transferability principle, a multipolar model is applied for the molecule and only the structural parameters (scale factor, atomic coordinates and displacement parameters) are refined. The Fourier residual maps are improved, notably on the covalent bonds, due to the proper electron-density modelling.

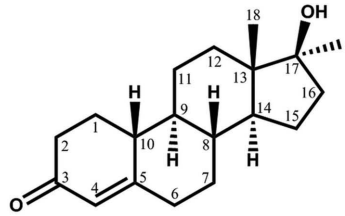

Methyloestrenolone

Aspergillus niger

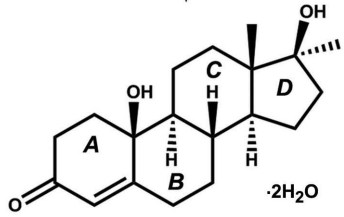

10β,17β-dihydroxy-17α-methylestr-4-en-3-one

(I)

During the current study, 10β,17β-dihydroxy-17α-methylestr-4-en-3-one dihydrate, (I) (see Scheme), was obtained from the fungal biotransformation of methyloestrenolone, a contraceptive agent (Zafar *et al.*, 2013; Yousuf *et al.*, 2010). The substrate belongs to the estrane class of compounds, steroids without the C-19 methyl group (Mason, 1948). Its structure has been investigated by single-crystal X-ray diffraction analysis and its molecular properties have been investigated using the electron-density parameters from the ELMAM2 library.

2. Experimental

2.1. Culture preparation

Aspergillus niger (ATCC 10549) was cultured in liquid media, prepared by dissolving glucose (10.0 g), peptone (5.0 g), yeast extract (3.0 g), KH_2PO_4 (5.0 g), glycerol (10.0 ml) and NaCl (5.0 g) per litre of distilled water. The media were sterilized followed by inoculation of the fungal spores. After optimum growth, methyloestrenolone (1.0 g) was transferred to the culture in the form of a solution in acetone (Zafar *et al.*, 2013).

2.2. Synthesis and crystallization

Incubation of methyloestrenolone was carried out for 14 d. The biomass was then separated by filtration and the filtrate was extracted with dichloromethane. The extract was subjected to column chromatography and size exclusion HPLC

(GS-320, MeOH, retention time = 33 min) to obtain 10β,17α-dihydroxy-17α-methylestr-4-en-3-one as a pure white crystalline solid. The yield of the reaction was only 0.08%. The single crystal used for X-ray diffraction analysis was chosen directly from the product.

2.3. Structure solution and refinement

Structure refinement details for the transferred model are summarized in Table 1. The structure was solved in the orthorhombic space group $P2_12_12_1$ using *SIR92* (Altomare *et al.*, 1993) available in the *WinGX* package (Farrugia, 2012). An initial IAM refinement was carried out using *SHELXL2013* (Sheldrick, 2015). Most of the H atoms were located in difference Fourier maps. However, H atoms on O atoms could not be ascertained in the difference Fourier maps and a riding model was thus used, as was employed for the H atoms attached to C atoms. After the initial cycles of refinement, the model was imported into *MoPro* (Jelsch *et al.*, 2005). An I/σ cut-off of 3 was applied throughout the *MoPro* refinements. The bond lengths for H atoms were constrained to standard neutron distances from the *International Tables of Crystallography* (Allen & Bruno, 2010).

2.3.1. IAM refinement. A full-matrix least-squares refinement was carried out against intensity data using *MoPro* (Jelsch *et al.*, 2005). A *SHELX*-type weighting scheme was adopted $\{w = 1/[\sigma^2(F_o^2) + (aP)^2 + bP]$, where $P = (F_o^2 + 2F_c^2)/3$, with $a = 0.1$ and $b = 0.01\}$ in order to have a goodness-of-fit close to unity. The *MoPro* software provides an easy way to modify the weighting scheme. The normal probability plots (Zhurov *et al.*, 2008) are shown in the *Supporting information* (Fig. S1). Initially, only the scale factor was refined. Subsequently, the positions and displacement parameters were also refined. The refinement was carried out until convergence. The anisotropic displacement parameters for H atoms were constrained to estimated values using the *SHADE* server (Madsen, 2006). The residual electron-density maps after the IAM refinement are available in the *Supporting information* (see Fig. S2*a*). It can be seen from the residual maps that the electron-density peaks reside on the covalent bonds and there are no significant residual density peaks on the atoms. At the end of the IAM refinement, the crystallographic R factor $R[F^2 > 2\sigma(F^2)]$ was 0.060, the weighted R factor $wR(F^2)$ was 0.149 and the goodness-of-fit S was 1.05. The minimum and maximum electron-density peaks after IAM refinement were −0.35 and 0.41 e Å^{-3}, respectively.

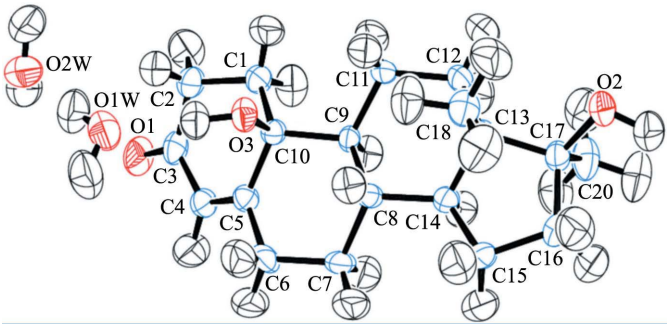

Figure 1
The molecular structure of the title compound, showing the atom-numbering scheme for the non-H atoms. Displacement ellipsoids are drawn at the 50% probability level.

Table 2
Hydrogen-bond geometry (Å, °).

D—H···A	D—H	H···A	D···A	D—H···A
O2W—H4W···O2^{i}	0.98	2.05	3.0279 (7)	176
O2W—H2W···O3^{ii}	0.98	1.82	2.7933 (6)	171
C14—H14A···C20	1.10	2.70	3.0951 (7)	101
C11—H11A···C1	1.09	2.59	2.9771 (8)	100
C18—H18A···C16	1.08	2.63	3.0340 (8)	102
C12—H12A···C20	1.09	2.60	3.0209 (8)	102
C2—H2B···O2W	1.09	2.69	3.5634 (7)	137
O1W—H1W···O2W	0.98	1.85	2.8189 (7)	169
O3—H3···O1W	0.98	1.79	2.7672 (6)	172
O1W—H3W···O2^{iii}	0.98	1.93	2.9053 (6)	172
O2—H2···O1^{iv}	0.98	1.77	2.7352 (6)	168
C6—H6B···O1^{v}	1.09	2.56	3.4828 (7)	141

Symmetry codes: (i) $x-1, y+1, z$; (ii) $x-\frac{1}{2}, -y+\frac{3}{2}, -z$; (iii) $x, y+1, z$; (iv) $x+1, y-1, z$; (v) $x+1, y, z$.

2.3.2. ELMAM2 refinement. The electron-density multipolar parameters of Hansen and Coppen's model (Hansen & Coppens, 1978) were transferred from the ELMAM2 library (Domagała *et al.*, 2012) using the built-in option in the *MoPro* software (Jelsch *et al.*, 2005). The molecule was neutralized electrically after the transfer. The electron-density parameters were kept fixed during the ELMAM2 refinement and only the scale factor, position and displacement parameters were refined until convergence. The anisotropic displacement parameters for H atoms were kept constrained to estimated values, as explained previously. The ELMAM2 refinement revealed a noticeable improvement in the refinement statistics; the crystallographic R factor $R[F^2 > 2\sigma(F^2)]$ was 0.048, the weighted R factor $wR(F^2)$ was 0.116 and the goodness-of-fit S was 0.95. The minimum and maximum electron-density peaks were −0.26 and 0.35 e Å^{-3}, respectively.

3. Results and discussion

The asymmetric unit of the title compound, (I) (Fig. 1), consists of one parent molecule along with two water molecules of crystallization, whereas the unit cell contains four parent molecules along with eight water molecules. The compound possesses the typical core structure of steroids, having three six-membered rings and a five-membered ring. The cyclohexene ring (A) is not planar in shape and adopts a half-chair conformation. Atoms C2, C3, C4 and C5 lie in the same plane. However, atom C1 deviates from the mean C2–C5 plane by 0.713 (2) Å, whereas atom C10 deviates from this plane by 0.218 (2) Å. The two central cyclohexane rings (B and C) both adopt a typical chair conformation, whereas cyclopentane ring D adopts a 13β,17α-envelope conformation (Cremer & Pople, 1975). The A/B ring junction is quasi-*trans*, whereas the B/C and C/D ring junctions both have a *trans* configuration (Bucourt, 1974). The torsion angle of the opposing methyl groups is −162.2 (2)°, as measured on C18—C13—C17—C20. All the bond lengths and angles are within

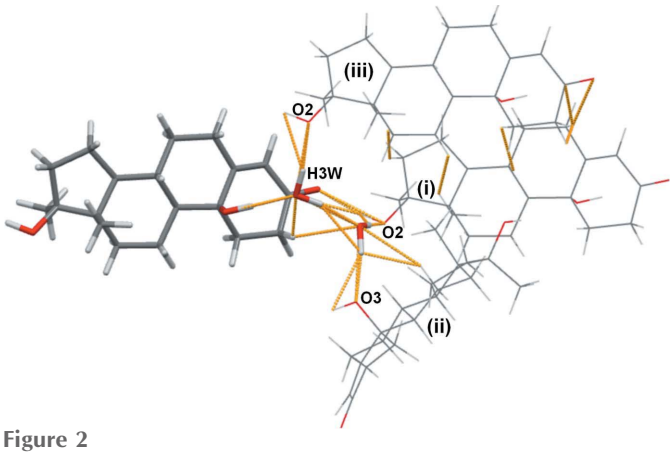

Figure 2
A view of the molecular assembly, showing the role of the water molecules in bridging together other molecules. The symmetry codes are the same as in Table 2. The bold sticks represent the asymmetric unit.

the normal range for similar structures (Galdecki *et al.*, 1990; Vasuki *et al.*, 2002; Thamotharan *et al.*, 2004; Shen *et al.*, 2011).

The molecular assembly is stabilized by strong intermolecular hydrogen bonds (Table 2), which are reinforced by a number of lateral weak H···H interactions. The primary aggregation motif is the O—H···O hydrogen bond between the C17 hydroxy donor and the O1 ketone acceptor (Duax & Norton, 1975), with an H···O distance of 1.77 Å and a *D*—H···*A* angle of 168°. This motif is typical of steroidal assemblies and results in the $P2_1$ or $P2_12_12_1$ space group. The two water molecules serve to bridge the molecular chains along three dimensions through strong intermolecular hydrogen bonding (Fig. 2). The O1*W* water molecule forms three strong O—H···O hydrogen bonds. Firstly, it donates its H3*W* atom to the O2^{iii} atom of the C17 hydroxy group (see Table 2 for the hydrogen-bond geometry and symmetry codes). Secondly, it accepts the H3 atom of the C10 hydroxy group. Thirdly, it donates atom H1*W* to the O2*W* atom of the other water molecule of the asymmetric unit. The O2*W* water molecule further links with two other neighbouring molecules by donating its H atoms to the O2^{i} and O3^{ii} atoms of the C17 and C10 hydroxy groups.

3.1. Hirshfeld surface analysis

The Hirshfeld surface emerged from an attempt to define the space occupied by a molecule in a crystal for the purpose of partitioning the crystal electron density into molecular fragments (Spackman & Byrom, 1997). The first function of distance explored for mapping on the surface involved the distances from the Hirshfeld surface to the adjacent nucleus inside (or internal, d_i) and outside (or external, d_e) the surface. By the informative use of these quantities, one can find a combination of d_i and d_e in the form of a two-dimensional fingerprint plot, which was invented due to the difficulty of representation in a two-dimensional format (printed page or computer monitor). Two different but potentially useful distance measurements each mapped on a three-dimensional molecular surface were invented. Surface features characteristic of different types of intermolecular interactions can be identified and such features can be exposed by colour coding distances from the surface to the nearest atom exterior or interior to the surface. In this study, d_e and d_i properties are calculated separately and an additional contact distance, d_{norm}, combines both d_e and d_i, each normalized by the van der Waals radius for the particular atoms involved in the close contact to the surface. Using a red–white–blue colour scheme to distinguish it from the red–green–blue schemes for d_e and d_i, contacts shorter than van der Waals separations show up as red spots on a largely blue surface. And because the definition of d_{norm} is symmetric in both d_e and d_i, close intermolecular contacts appear as three identical red spots (but not neces-

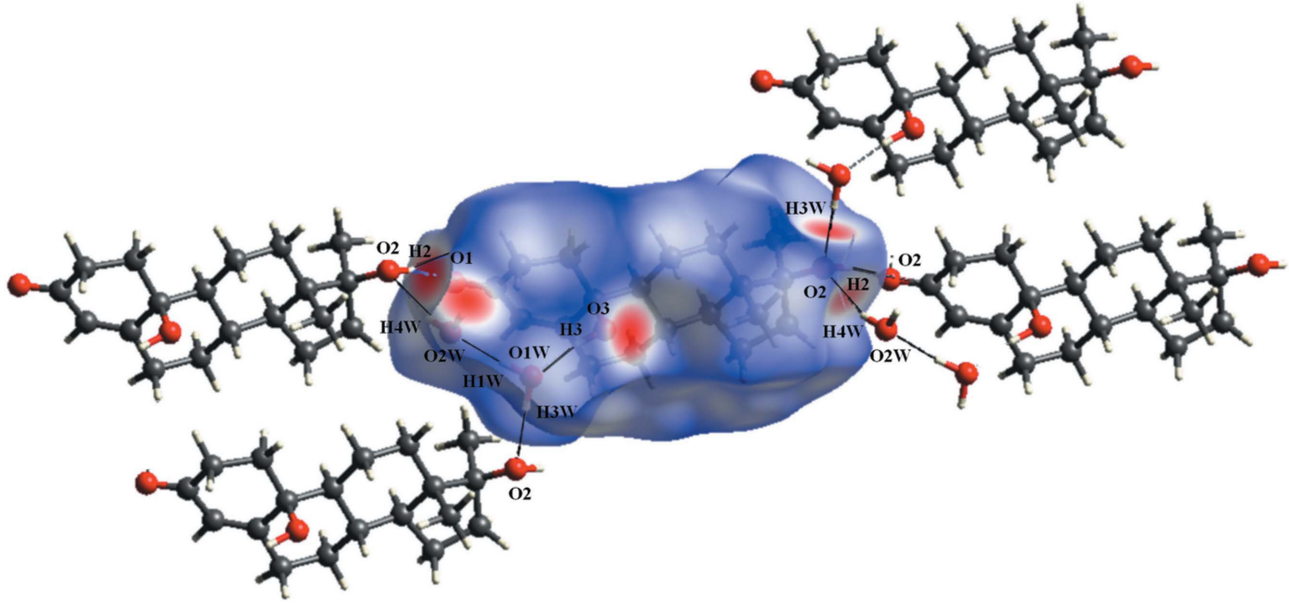

Figure 3
A Hirshfeld surface of the parent molecule, showing the interacting molecules. Generic atom labels without symmetry codes are given.

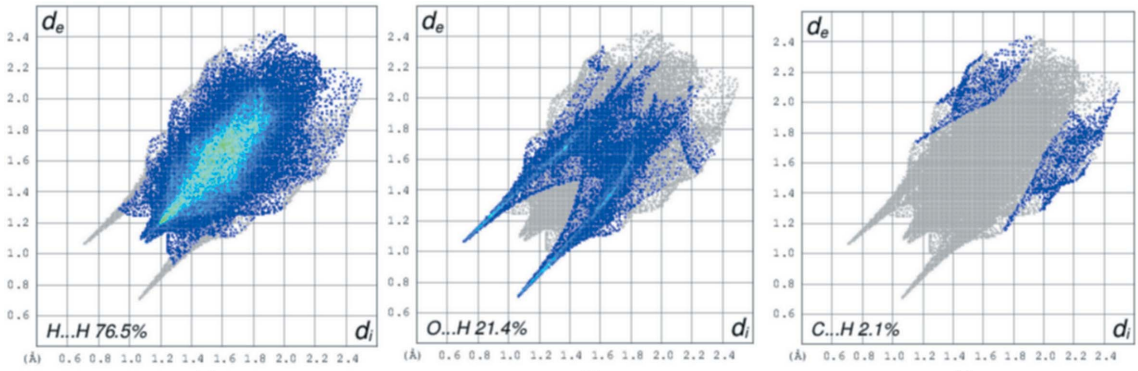

(*a*) (*b*) (*c*)

Figure 4
Fingerprint plots of the title compound, showing the percentage of various interactions.

sarily on the same molecule if there is more than one molecule in the asymmetric unit) (Spackman & Jayatilaka, 2009).

Crystal Explorer 3.1 (Wolff *et al.*, 2012) was used to generate Hirshfeld surfaces mapped over the d_{norm} property of the molecule. It is seen that the hydrogen bond between carbonyl atom O1 and water atom H2*W* is associated with large red spots, while the alcohol groups present on the ring making intermolecular contacts are shown by the regions coloured in red (Fig. 3).

The fingerprint plots (Fig. 4) of the structure support the intermolecular interactions. Three types of interactions are found in the crystal packing: H···H interactions account for 76.5%, O···H for 21.4% and C···H for 2.1%. Calculation of the enrichment ratio (ER) (Jelsch *et al.*, 2014) shows that the H···H contacts are relatively more favoured, with an ER value of 1.13, over O···H and C···H interactions, whose ER values are 0.566 and 0.565, respectively.

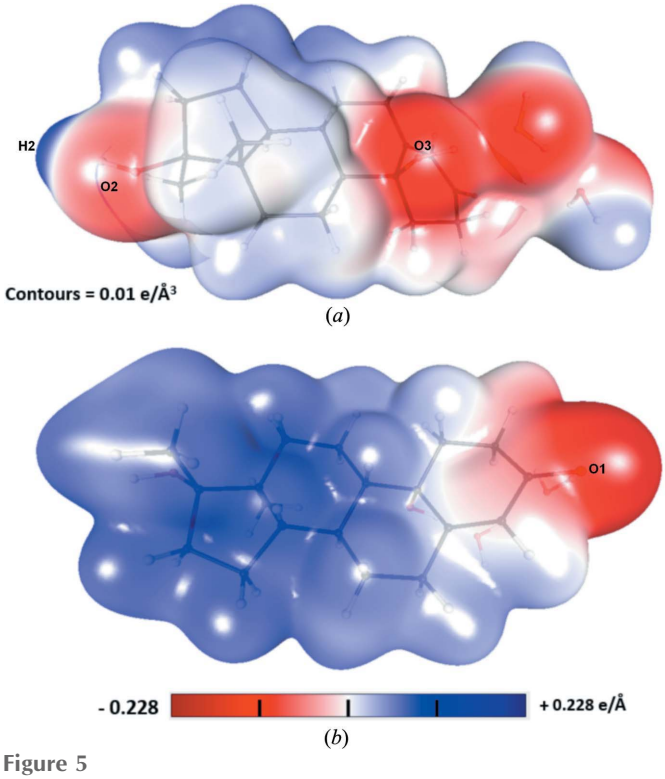

(*a*) (*b*)

Figure 5
A three-dimensional electron-density isosurface generated at an electron-density value of 0.01 e Å^{-3}, coloured according to the electrostatic potential.

3.2. Electrostatic potential and the dipole moment

The presence of possible electrostatic interactions around the molecule can be described qualitatively by the electrostatic potential map (ESP) on the electron-density isosurface. The electrostatic potential can be calculated directly from the electron density (Su & Coppens, 1992). The electrostatic potential mapped on the isosurface of electron density had a value of 0.01 e Å^{-3}; Fig. 5 shows two views of the three-dimensional electron-density surface coloured according to the electrostatic potential. Fig. 5(*a*) shows a projection of the molecule with the hydroxy groups projected towards the viewer, whereas in Fig. 5(*b*), the molecule is rotated to show it downwards. The maps show that around all the three O atoms there is an accumulation of electron density. Atom H2 of the hydroxy group has a strong positive region. The carbonyl O1 atom has the greatest concentration of negative charge. In fact, this is the reason behind the polar nature of the compound, as evident from the relatively high dipole moment value (10.09 Debye) of the molecule (Fig. 6). The dipole moment was calculated for an electrically neutralized molecule using *MoProViewer* (Guillot, 2011), with the origin at the coordinate centre, and is the sum of the dipolar contributions only. The polar nature of the molecule also results in the typical head-to-tail arrangement in the crystal structure. During the process of biotransformation, the H atom on C10 is replaced by the O3 hydroxy group, which has an accumulation of negative charge. Since electrostatic forces are long-range forces, molecules can recognize each other from a distance. These negative electrostatic regions can be potential binding sites for hydrogen bonds and for attack by electrophilic species. It can be said with confidence that the binding mode of the biotransformed product will certainly be different from that of its parent molecule methyloestrenolone.

The topography of the electrostatic potential in the molecule under study is significantly different from that of the estrone molecule (Zhurova *et al.*, 2006) due to the opposite

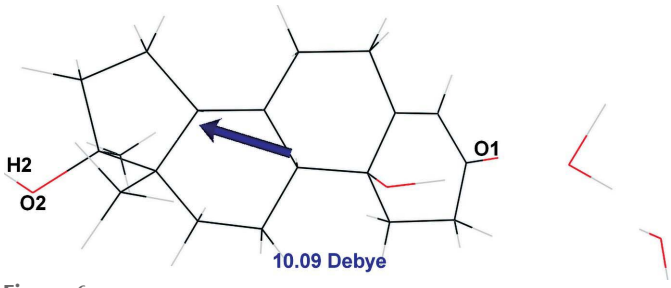

Figure 6
The total dipole moment of (I), computed on the basis of transferred parameters.

locations of the carbonyl O atom and the hydroxy group in the two molecules. The addition of the O3 hydroxy group in the current study renders the *syn* sides of rings *A*, *B* and *C* significantly negative or neutral, whereas the *anti* sides of the rings are electrostatically more positive. Ring *D* has the greatest concentration of positive potential. The same has been indicated by the direction of the dipole moment vector.

3.3. Topology of intermolecular interactions

A quantitative analysis of the intermolecular interactions of the title molecule was carried out on the basis of topological analysis using the Bader quantum theory of atoms in molecules (Bader, 1990). The literature reports the successful use of the transferability principle to precisely quantify the electron-density-derived properties for the crystals which diffract to ordinary resolutions (Domagała *et al.* 2011; Bibila Mayaya Bisseyou *et al.*, 2012; Dadda *et al.*, 2012). All three O atoms of the parent molecule are involved in the formation of O—H···O hydrogen-bond interactions at very short distances of less than 2 Å. The electron-density values at the critical points are significantly greater than other types of interactions. Moreover, the presence of 3,-1-type bond-critical points and a positive Laplacian value establish that they are strong hydrogen bonds. Table S1 (see *Supporting information*) gives the topological parameters of the intermolecular interactions.

4. Conclusion

This paper reports the crystal structure and charge–density properties of a molecule which was obtained as a biotransformation product of the steroid drug methylestrenolone. The structure is stabilized by a number of O—H···O and C—H···O hydrogen bonds which are assisted by a number H···H interactions. Even though the diffraction data were limited to ordinary resolution, the charge–density properties, electrostatic potential, dipole moment and topology of intermolecular interactions could be estimated using the transferred parameters from the ELMAM2 database. The results show that the ELMAM2 model is better. The procedure is very rapid and simplified in the *MoPro* software, although it may require some manual intervention. The method is very suitable for the high throughput screening of diverse targets, especially biologically active molecules, if diffraction data is available.

Acknowledgements

The authors greatly acknowledge the ICCBS, University of Karachi, for providing the X-ray diffraction facility.

References

Ahmad, M. S., Zafar, S., Bibi, M., Bano, S. & Choudhary, M. I. (2014). *Steroids*, **82**, 53–59.
Ahmed, M., Noureen, S., Gros, P. C., Guillot, B. & Jelsch, C. (2011). *Acta Cryst.* C**67**, o329–o333.
Allen, F. H. & Bruno, I. J. (2010). *Acta Cryst.* B**66**, 380–386.
Altomare, A., Cascarano, G., Giacovazzo, C. & Guagliardi, A. (1993). *J. Appl. Cryst.* **26**, 343–350.
Bader, R. F. W. (1990). In *Atoms in Molecules – A Quantum Theory*. Oxford University Press.
Bucourt, R. (1974). *The Torsion Angle Concept in Conformational Analysis*, in *Topics in Stereochemistry*, edited by E. L. Eliel & N. L. Allinger, Vol. 8, p. 159. New York: Interscience.
Bibila Mayaya Bisseyou, Y., Bouhmaida, N., Guillot, B., Lecomte, C., Lugan, N., Ghermani, N. & Jelsch, C. (2012). *Acta Cryst.* B**68**, 646–660.
Brock, C. P., Dunitz, J. D. & Hirshfeld, F. L. (1991). *Acta Cryst.* B**47**, 789–797.
Bruker (2000). *SADABS*, *SMART* and *SAINT*. Bruker AXS Inc., Madison, Wisconsin, USA.
Cao, H., Chen, X., Jassbi, A. R. & Xiao, J. (2015). *Biotechnol. Adv.* **33**, 214–223.
Choudhary, M. I., Zafar, S., Khan, N. T., Ahmad, S., Noreen, S., Marasini, B. P., Al-Khedhairy, A. A. & Atta-ur-Rahman (2012). *J. Enz. Inhib. Med. Chem.* **27**, 348–355.
Coppens, P. (1998). *Acta Cryst.* A**54**, 779–788.
Cremer, D. & Pople, J. A. (1975). *J. Am. Chem. Soc.* **97**, 1354–1358.
Dadda, N., Nassour, A., Guillot, B., Benali-Cherif, N. & Jelsch, C. (2012). *Acta Cryst.* A**68**, 452–463.
Dittrich, B., Hübschle, C. B., Messerschmidt, M., Kalinowski, R., Girnt, D. & Luger, P. (2005). *Acta Cryst.* A**61**, 314–320.
Dittrich, B., Koritsànszky, T. & Luger, P. (2004). *Angew. Chem. Int. Ed.* **43**, 2718–2721.
Dittrich, B., Munshi, P. & Spackman, M. A. (2007). *Acta Cryst.* B**63**, 505–509.
Domagała, S., Fournier, B., Liebschner, D., Guillot, B. & Jelsch, C. (2012). *Acta Cryst.* A**68**, 337–351.
Domagała, S. & Jelsch, C. (2008). *J. Appl. Cryst.* **41**, 1140–1149.
Domagała, S., Munshi, P., Ahmed, M., Guillot, B. & Jelsch, C. (2011). *Acta Cryst.* B**67**, 63–78.
Duax, W. L. & Norton, D. A. (1975). In *Atlas of Steroid Structures*. New York: Plenum.
Farrugia, L. J. (2012). *J. Appl. Cryst.* **45**, 849–854.
Galdecki, Z., Grochulski, P. & Wawrzak, Z. (1990). *J. Crystallogr. Spectrosc. Res* **20**, 425–428.
Guillot, B. (2011). *Acta Cryst.* A**67**, C511–C512.
Guillot, B., Viry, L., Guillot, R., Lecomte, C. & Jelsch, C. (2001). *J. Appl. Cryst.* **34**, 214–223.
Hansen, N. K. & Coppens, P. (1978). *Acta Cryst.* A**34**, 909–921.
Hirshfeld, F. L. (1976). *Acta Cryst.* A**32**, 239–244.
Holland, H. L. (1999). *Steroids*, **64**, 178–186.
Jayatilaka, D. (2012). *Modern Charge-Density Analysis*, edited by C. Gatti & P. Macchi, pp. 213–257. New York: Springer.
Jelsch, C., Ejsmont, K. & Huder, L. (2014). *IUCrJ*, **1**, 119–128.
Jelsch, C., Guillot, B., Lagoutte, A. & Lecomte, C. (2005). *J. Appl. Cryst.* **38**, 38–54.

Jelsch, C., Pichon-Pesme, V., Lecomte, C. & Aubry, A. (1998). *Acta Cryst.* D**54**, 1306–1318.
Khan, N. T., Zafar, S., Noreen, S., Al Majid, A. M., Al Othman, Z. A., Al-Resayes, S. I. & Choudhary, M. I. (2014). *Steroids*, **85**, 65–72.
Leon, R., Fernandes, P., Pinheiro, H. & Cabral, J. (1998). *Enzyme Microb. Technol.* **23**, 483–500.
Liu, J.-H. & Yu, B.-Y. (2010). *Curr. Org. Chem*. **14**, 1400–1406.
Macrae, C. F., Edgington, P. R., McCabe, P., Pidcock, E., Shields, G. P., Taylor, R., Towler, M. & van de Streek, J. (2006). *J. Appl. Cryst.* **39**, 453–457.
Madsen, A. Ø. (2006). *J. Appl. Cryst.* **39**, 757–758.
Mahato, S. B. & Garai, S. (1997). *Steroids*, **62**, 332–345.
Mason, H. L. (1948). *J. Clin. Endocrinol. Metab.* **8**, 190–205.
Monagas, M., Urpi-Sarda, M., Sánchez-Patán, F., Llorach, R., Garrido, I., Gómez-Cordovés, C., Andres-Lacueva, C. & Bartolomé, B. (2010). *Food Function*, **1**, 233–253.
Palomo, J. M. & Filice, M. (2015). *Biotechnol. Adv*. **33**, 605–613.
Pichon-Pesme, V., Lecomte, C. & Lachekar, H. (1995). *J. Phys. Chem*. **99**, 6242–6250.
Ruysink, A. F. J. & Vos, A. (1974). *Acta Cryst.* A**30**, 503–506.
Sheldrick, G. M. (2015). *Acta Cryst.* C**71**, 3–8.
Shen, Y.-B., Wang, M., Liang, Q.-K. & Luo, J. (2011). *Acta Cryst.* E**67**, o2752.
Spackman, M. A. & Byrom, P. G. (1997). *Chem. Phys. Lett*. **267**, 215–220.
Spackman, M. A. & Jayatilaka, D. (2009). *CrystEngComm*, **11**, 19–32.
Su, Z. & Coppens, P. (1992). *Acta Cryst.* A**48**, 188–197.
Thamotharan, S., Parthasarathi, V., Dubey, S., Jindal, D. P. & Linden, A. (2004). *Acta Cryst.* C**60**, o110–o112.
Vasuki, G., Parthasarathi, V., Ramamurthi, K., Dubey, S. & Jindal, D. P. (2002). *Acta Cryst.* E**58**, o1359–o1360.
Wang, M.-X. (2015). *Acc. Chem. Res*. **48**, 602–611.
Wang, M.-X., Lu, G., Ji, G.-J., Huang, Z.-T., Meth-Cohn, O. & Colby, J. (2000). *Tetrahedron Asymmetry*, **11**, 1123–1135.
Westrip, S. P. (2010). *J. Appl. Cryst.* **43**, 920–925.
Wolff, S. K., Grimwood, D. J., McKinnon, J. J., Turner, M. J., Jayatilaka, D. & Spackman, M. A. (2012). *Crystal Explorer*. The University of Western Australia.
Yousuf, S., Zafar, S., Choudhary, M. I. & Ng, S. W. (2010). *Acta Cryst.* E**66**, o2894.
Zafar, S., Bibi, M., Yousuf, S. & Choudhary, M. I. (2013). *Steroids*, **78**, 418–425.
Zafar, S., Yousuf, S., Kayani, H. A., Saifullah, S., Khan, S., Al-Majid, A. M. & Choudhary, M. I. (2012). *Chem. Cent. J.* **6**, 109–116.
Zarychta, B., Pichon-Pesme, V., Guillot, B., Lecomte, C. & Jelsch, C. (2007). *Acta Cryst.* A**63**, 108–125.
Zhurova, E. A., Matta, C. F., Wu, N., Zhurov, V. & Pinkerton, A. A. (2006). *J. Am. Chem. Soc.* **128**, 8849–8861.
Zhurov, V. V., Zhurova, E. A. & Pinkerton, A. A. (2008). *J. Appl. Cryst.* **41**, 340–349.

supporting information

Acta Cryst. (2016). C**72**, 398-404 [doi:10.1107/S2053229616005441]

Transferred multipolar atom model for 10β,17β-dihydroxy-17α-methylestr-4-en-3-one dihydrate obtained from the biotransformation of methyloestrenolone

Muhammad Umer Faroque, Sammer Yousuf, Salman Zafar, M. Iqbal Choudhary and Maqsood Ahmed

Computing details

Data collection: *SMART* (Bruker, 2000); cell refinement: *SAINT* (Bruker, 2000); data reduction: *SAINT* (Bruker, 2000); program(s) used to solve structure: *SIR92* (Altomare *et al.*, 1993); program(s) used to refine structure: MoPro (Jelsch *et al.*, 2005); molecular graphics: *Mercury* (Macrae *et al.*, 2006) and *MoProViewer* (Guillot, 2011); software used to prepare material for publication: pubCIF (Westrip, 2010).

17α-Methyl-10β,17β-dihydroxyestr-4-en-3-one dihydrate

Crystal data

$C_{19}H_{28}O_3 \cdot 2H_2O$
$M_r = 340.44$
Orthorhombic, $P2_12_12_1$
Hall symbol: P 2ac 2ab
$a = 6.9028$ (6) Å
$b = 11.0334$ (10) Å
$c = 24.451$ (2) Å
$V = 1862.2$ (3) Å^3
$Z = 4$
$F(000) = 744$
$D_x = 1.215$ Mg m^{-3}
Mo $K\alpha$ radiation, $\lambda = 0.71073$ Å
Cell parameters from 507 reflections
$\theta = 2.0$–$28.3°$
$\mu = 0.09$ mm^{-1}
$T = 100$ K
Block, colorless
0.27 × 0.10 × 0.07 mm

Data collection

Bruker SMART CCD detector diffractometer
Radiation source: fine-focus sealed tube
Graphite monochromator
ω and phi scan
Absorption correction: multi-scan (*SADABS*; Bruker, 2000)
$T_{min} = 0.977$, $T_{max} = 0.994$
13666 measured reflections
2792 independent reflections
2792 reflections with $> 2.0\sigma(I)$
$R_{int} = 0.052$
$\theta_{max} = 28.3°$, $\theta_{min} = 2.0°$
$h = 0 \rightarrow 9$
$k = 0 \rightarrow 14$
$l = -31 \rightarrow 32$

Refinement

Refinement on F^2
Least-squares matrix: full
$R[F^2 > 2\sigma(F^2)] = 0.048$
$wR(F^2) = 0.116$
$S = 0.95$
2792 reflections
217 parameters
0 restraints
Primary atom site location: structure-invariant direct methods
Secondary atom site location: difference Fourier map
Hydrogen site location: difference Fourier map
H-atom parameters constrained
$w = 1/[\sigma^2(F_o^2) + (0.08P)^2 + 0.01P]$ where $P = (F_o^2 + 2F_c^2)/3$

$(\Delta/\sigma)_{max}$ = 0.029
$\Delta\rho_{max}$ = 0.35 e Å^{-3}
$\Delta\rho_{min}$ = −0.26 e Å^{-3}

Special details

Refinement. Refinement of F^2 against reflections. The threshold expression of $F^2 > 2\text{sigma}(F^2)$ is used for calculating R-factors(gt) and is not relevant to the choice of reflections for refinement. R-factors based on F^2 are statistically about twice as large as those based on F, and R-factors based on ALL data will be even larger.

Fractional atomic coordinates and isotropic or equivalent isotropic displacement parameters (Å^2)

	x	*y*	*z*	U_{iso}*/U_{eq}
O2	0.8602 (3)	0.00169 (19)	0.10105 (8)	0.0423 (3)
O3	0.5688 (3)	0.60762 (16)	0.06832 (8)	0.0372 (3)
C9	0.5046 (4)	0.4361 (2)	0.12707 (11)	0.0256 (4)
H9A	0.41191	0.40931	0.16156	0.04780
C14	0.7637 (4)	0.2990 (2)	0.16183 (11)	0.0294 (4)
H14A	0.66047	0.27174	0.19375	0.05083
C5	0.4790 (4)	0.6495 (3)	0.16041 (11)	0.0307 (4)
C8	0.7149 (4)	0.4297 (3)	0.14791 (11)	0.0284 (4)
H8A	0.81266	0.46121	0.11542	0.04817
C11	0.4658 (5)	0.3443 (3)	0.08087 (12)	0.0331 (4)
H11A	0.31178	0.34602	0.07072	0.05949
H11B	0.54685	0.37136	0.04450	0.05485
C10	0.4443 (4)	0.5670 (2)	0.11168 (11)	0.0281 (4)
C7	0.7392 (5)	0.5118 (3)	0.19804 (12)	0.0416 (5)
H7A	0.65417	0.47503	0.23184	0.06419
H7B	0.89122	0.51245	0.21040	0.06902
C13	0.7357 (4)	0.2086 (2)	0.11473 (10)	0.0264 (4)
C18	0.8680 (5)	0.2376 (3)	0.06591 (12)	0.0406 (5)
H18A	1.01710	0.23352	0.07871	0.06905
H18B	0.84316	0.17249	0.03384	0.07116
H18C	0.83579	0.32719	0.05098	0.06451
C12	0.5237 (4)	0.2144 (3)	0.09678 (13)	0.0342 (4)
H12A	0.43130	0.18307	0.13014	0.05931
H12B	0.50184	0.15422	0.06188	0.06311
O1	0.0599 (4)	0.8371 (2)	0.16287 (11)	0.0586 (4)
C17	0.8069 (5)	0.0905 (3)	0.14221 (12)	0.0335 (4)
C1	0.2322 (5)	0.5695 (3)	0.09338 (13)	0.0383 (4)
H1A	0.22059	0.53019	0.05251	0.06126
H1B	0.14759	0.51247	0.12100	0.06175
C15	0.9659 (5)	0.2692 (3)	0.18443 (13)	0.0415 (4)
H15A	0.97576	0.29139	0.22786	0.07100
H15B	1.07860	0.31790	0.16212	0.06733
C4	0.3475 (5)	0.7313 (3)	0.17698 (12)	0.0373 (5)
H4A	0.38181	0.78734	0.21204	0.06920
C6	0.6738 (5)	0.6412 (3)	0.18718 (13)	0.0398 (5)
H6A	0.66908	0.68972	0.22609	0.07267
H6B	0.78006	0.68447	0.16047	0.06481

C3	0.1726 (5)	0.7590 (3)	0.14602 (13)	0.0415 (5)
C2	0.1439 (5)	0.6959 (3)	0.09252 (13)	0.0422 (5)
H2B	0.21031	0.74961	0.06003	0.06146
H2C	−0.01102	0.68996	0.08388	0.07212
C20	0.6574 (6)	0.0294 (3)	0.17962 (15)	0.0538 (6)
H20A	0.61344	0.09206	0.21101	0.07347
H20B	0.53306	0.00390	0.15564	0.07587
H20C	0.72042	−0.05018	0.19795	0.07833
C16	0.9857 (5)	0.1317 (3)	0.17549 (14)	0.0492 (6)
H16A	0.99000	0.08430	0.21468	0.06984
H16B	1.11854	0.11132	0.15304	0.06804
O2W	0.2174 (4)	0.9836 (2)	0.02964 (10)	0.0615 (4)
O1W	0.5632 (4)	0.8548 (2)	0.04914 (11)	0.0612 (4)
H3W	0.65624	0.91064	0.06619	0.07568
H2W	0.16287	0.96002	−0.00594	0.08736
H1W	0.45287	0.90897	0.04218	0.07005
H4W	0.10077	0.99330	0.05231	0.07847
H2	0.91659	−0.06430	0.12264	0.06365
H3	0.55537	0.69538	0.06344	0.05217

Atomic displacement parameters (Å²)

	U^{11}	U^{22}	U^{33}	U^{12}	U^{13}	U^{23}
O2	0.0494 (14)	0.0297 (10)	0.0477 (12)	0.0106 (10)	−0.0023 (11)	−0.0037 (10)
O3	0.0495 (13)	0.0286 (10)	0.0335 (10)	0.0054 (9)	0.0103 (10)	0.0027 (9)
C9	0.0251 (14)	0.0208 (13)	0.0310 (13)	0.0023 (11)	−0.0025 (12)	0.0023 (11)
H9A	0.04670	0.04902	0.04769	0.00082	0.01143	0.00489
C14	0.0318 (15)	0.0293 (15)	0.0271 (13)	0.0026 (12)	−0.0014 (13)	−0.0015 (12)
H14A	0.05833	0.05167	0.04248	0.00608	0.00709	0.00416
C5	0.0324 (15)	0.0295 (14)	0.0302 (14)	0.0019 (13)	0.0011 (13)	−0.0017 (12)
C8	0.0258 (15)	0.0297 (14)	0.0298 (13)	0.0016 (12)	−0.0043 (13)	−0.0050 (12)
H8A	0.04245	0.04858	0.05347	−0.00291	0.00583	0.00180
C11	0.0363 (17)	0.0274 (14)	0.0354 (15)	0.0027 (13)	−0.0138 (14)	−0.0047 (12)
H11A	0.04853	0.05005	0.07988	0.00065	−0.01864	−0.00748
H11B	0.07035	0.05036	0.04386	0.00319	0.00206	−0.00255
C10	0.0280 (15)	0.0282 (14)	0.0280 (13)	0.0042 (13)	−0.0018 (12)	−0.0013 (12)
C7	0.047 (2)	0.0402 (17)	0.0380 (16)	0.0112 (16)	−0.0182 (16)	−0.0155 (14)
H7A	0.08819	0.05911	0.04526	0.01453	−0.00217	−0.00440
H7B	0.06547	0.05982	0.08177	0.01011	−0.03232	−0.01591
C13	0.0279 (15)	0.0260 (14)	0.0254 (13)	0.0023 (12)	−0.0006 (12)	−0.0006 (11)
C18	0.0470 (19)	0.0396 (17)	0.0351 (15)	0.0078 (15)	0.0107 (15)	0.0018 (14)
H18A	0.05183	0.08156	0.07376	0.01050	0.01130	0.00585
H18B	0.09546	0.06445	0.05357	0.00781	0.01251	−0.01428
H18C	0.07743	0.05273	0.06337	0.01619	0.02049	0.00983
C12	0.0330 (16)	0.0255 (14)	0.0441 (17)	−0.0008 (13)	−0.0098 (14)	−0.0035 (13)
H12A	0.05198	0.05114	0.07481	−0.00202	0.00570	0.00851
H12B	0.07347	0.04768	0.06819	0.00511	−0.01940	−0.01524
O1	0.0635 (16)	0.0445 (13)	0.0679 (15)	0.0312 (12)	0.0027 (14)	−0.0031 (12)

C17	0.0392 (17)	0.0268 (14)	0.0345 (14)	0.0059 (13)	0.0000 (14)	0.0005 (12)
C1	0.0348 (17)	0.0327 (16)	0.0475 (17)	0.0057 (15)	−0.0096 (16)	−0.0017 (14)
H1A	0.06418	0.05552	0.06409	0.00766	−0.02065	−0.01060
H1B	0.04541	0.05408	0.08575	0.00055	0.00393	0.00879
C15	0.0399 (17)	0.0381 (16)	0.0465 (17)	0.0102 (15)	−0.0190 (16)	−0.0064 (15)
H15A	0.08518	0.06620	0.06163	0.02104	−0.02708	−0.01164
H15B	0.04933	0.05954	0.09310	0.00426	−0.00746	0.00014
C4	0.0448 (19)	0.0311 (15)	0.0359 (16)	0.0092 (15)	−0.0003 (15)	−0.0048 (13)
H4A	0.09336	0.06189	0.05236	0.02363	−0.00845	−0.01741
C6	0.0430 (18)	0.0276 (14)	0.0488 (17)	0.0035 (14)	−0.0079 (16)	−0.0134 (14)
H6A	0.09630	0.05963	0.06208	0.01900	−0.02904	−0.02275
H6B	0.05807	0.05270	0.08365	−0.00254	−0.01302	−0.00184
C3	0.0444 (18)	0.0332 (16)	0.0468 (18)	0.0137 (15)	0.0036 (16)	0.0044 (15)
C2	0.0424 (19)	0.0380 (17)	0.0463 (19)	0.0111 (15)	−0.0049 (16)	0.0007 (15)
H2B	0.07258	0.04982	0.06200	0.00514	−0.00692	0.00162
H2C	0.04959	0.06202	0.10476	0.00974	−0.01822	−0.00654
C20	0.069 (2)	0.0359 (18)	0.057 (2)	0.0068 (17)	0.016 (2)	0.0145 (16)
H20A	0.09266	0.05593	0.07182	0.00811	0.02421	0.00423
H20B	0.06954	0.06561	0.09246	−0.00867	−0.00135	0.01070
H20C	0.08983	0.05419	0.09097	0.01843	0.01026	0.02473
C16	0.056 (2)	0.0384 (17)	0.0535 (19)	0.0143 (16)	−0.0180 (18)	0.0025 (16)
H16A	0.08864	0.06098	0.05989	0.01685	−0.01541	0.00370
H16B	0.05549	0.06438	0.08425	0.01446	−0.00074	−0.00796
O2W	0.0669 (18)	0.0622 (16)	0.0553 (14)	0.0038 (14)	−0.0199 (13)	−0.0031 (13)
O1W	0.0709 (17)	0.0379 (12)	0.0749 (16)	−0.0040 (13)	−0.0093 (15)	0.0007 (12)
H3W	0.07694	0.04788	0.10221	−0.00752	0.00251	0.00962
H2W	0.12730	0.06475	0.07003	0.02179	−0.02287	0.00288
H1W	0.08313	0.04872	0.07831	0.00997	−0.00116	0.01020
H4W	0.09507	0.05961	0.08073	0.01899	−0.01069	−0.00002
H2	0.07789	0.04661	0.06645	0.01823	−0.00426	−0.00233
H3	0.06254	0.04085	0.05312	0.00376	0.00532	0.00679

Geometric parameters (Å, º)

O2—C17	1.4520 (12)	C18—H18B	1.0770
O2—H2	0.9800	C12—H12B	1.0920
O3—C10	1.4364 (12)	C12—H12A	1.0920
O3—H3	0.9800	O1—C3	1.2325 (15)
C9—C10	1.5493 (12)	C17—C16	1.5462 (15)
C9—C8	1.5400 (12)	C17—C20	1.5354 (15)
C9—C11	1.5407 (12)	C1—C2	1.5226 (14)
C9—H9A	1.0990	C1—H1A	1.0920
C14—C13	1.5360 (12)	C1—H1B	1.0920
C14—C8	1.5192 (13)	C15—C16	1.5387 (15)
C14—C15	1.5364 (14)	C15—H15A	1.0920
C14—H14A	1.0990	C15—H15B	1.0920
C5—C10	1.5181 (13)	C4—C3	1.4572 (16)
C5—C6	1.4979 (14)	C4—H4A	1.0830

C5—C4	1.3433 (15)	C6—H6A	1.0920
C8—C7	1.5335 (13)	C6—H6B	1.0920
C8—H8A	1.0990	C3—C2	1.4950 (15)
C11—C12	1.5380 (13)	C2—H2B	1.0920
C11—H11A	1.0920	C2—H2C	1.0920
C11—H11B	1.0920	C20—H20A	1.0770
C10—C1	1.5314 (14)	C20—H20C	1.0770
C7—C6	1.5210 (14)	C20—H20B	1.0770
C7—H7A	1.0920	C16—H16A	1.0920
C7—H7B	1.0920	C16—H16B	1.0920
C13—C17	1.5459 (12)	O2W—H4W	0.9830
C13—C12	1.5289 (14)	O2W—H2W	0.9830
C13—C18	1.5366 (13)	O1W—H1W	0.9830
C18—H18A	1.0770	O1W—H3W	0.9830
C18—H18C	1.0770		

C17—O2—H2	103.235	C17—C13—C12	117.7 (10)
C10—O3—H3	109.961	C17—C13—C18	108.9 (9)
C10—C9—C8	112.1 (9)	C12—C13—C18	109.7 (10)
C10—C9—C11	112.8 (9)	H18A—C18—H18C	109.504
C10—C9—H9A	106.331	H18A—C18—H18B	109.624
C8—C9—C11	112.1 (9)	H18C—C18—H18B	109.438
C8—C9—H9A	106.400	H12B—C12—H12A	108.064
C11—C9—H9A	106.529	C16—C17—C20	111 (1)
C13—C14—C8	114.9 (9)	C2—C1—H1A	108.756
C13—C14—C15	104.2 (9)	C2—C1—H1B	108.792
C13—C14—H14A	105.832	H1A—C1—H1B	107.362
C8—C14—C15	119.1 (10)	C16—C15—H15A	110.737
C8—C14—H14A	105.953	C16—C15—H15B	110.551
C15—C14—H14A	105.958	H15A—C15—H15B	109.310
C10—C5—C6	116.6 (10)	C3—C4—C5	123 (1)
C10—C5—C4	122 (1)	C3—C4—H4A	118.236
C6—C5—C4	121 (1)	H6A—C6—H6B	109.074
C7—C8—H8A	108.869	C2—C3—C4	118 (1)
C12—C11—H11A	109.041	H2B—C2—H2C	107.637
C12—C11—H11B	109.094	H20A—C20—H20C	109.926
H11A—C11—H11B	108.011	H20A—C20—H20B	109.307
C6—C7—H7A	108.739	H20C—C20—H20B	109.621
C6—C7—H7B	109.115	H16A—C16—H16B	108.643
H7A—C7—H7B	108.026	H4W—O2W—H2W	102.395
C17—C13—C14	100.4 (8)	H1W—O1W—H3W	101.439

O2—C17—C13—C14	−159.4 (5)	H8A—C8—C7—H7B	−56.03
O2—C17—C13—C12	83.8 (2)	C11—C9—C10—C1	54.5 (2)
O2—C17—C13—C18	−41.8 (2)	C11—C9—C8—C7	−173.4 (2)
O2—C17—C16—C15	139.8 (4)	C11—C12—C13—C17	168.8 (2)
O2—C17—C16—H16A	−100.15	C11—C12—C13—C18	−66.0 (2)
O2—C17—C16—H16B	19.66	H11A—C11—C9—C10	−58.29

O2—C17—C20—H20A	179.95
O2—C17—C20—H20C	59.39
O2—C17—C20—H20B	−60.58
O3—C10—C9—C8	61.4 (2)
O3—C10—C9—C11	−66.3 (2)
O3—C10—C9—H9A	177.29
O3—C10—C5—C6	−67.3 (2)
O3—C10—C5—C4	108.7 (2)
O3—C10—C1—C2	−76.7 (2)
O3—C10—C1—H1A	45.09
O3—C10—C1—H1B	161.98
C9—C10—O3—H3	−166.84
C9—C10—C5—C6	49.4 (2)
C9—C10—C5—C4	−134.6 (3)
C9—C10—C1—C2	164.1 (2)
C9—C10—C1—H1A	−74.19
C9—C10—C1—H1B	42.70
C9—C8—C14—C13	56.4 (2)
C9—C8—C14—C15	−179.1 (2)
C9—C8—C14—H14A	−60.03
C9—C8—C7—C6	−53.9 (2)
C9—C8—C7—H7A	66.79
C9—C8—C7—H7B	−175.31
C9—C11—C12—C13	−55.6 (2)
C9—C11—C12—H12B	−176.51
C9—C11—C12—H12A	65.24
H9A—C9—C10—C5	60.97
H9A—C9—C10—C1	−61.91
H9A—C9—C8—C14	64.47
H9A—C9—C8—C7	−57.37
H9A—C9—C8—H8A	−176.59
H9A—C9—C11—C12	−62.98
H9A—C9—C11—H11A	58.02
H9A—C9—C11—H11B	175.77
C14—C13—C17—C16	−40.3 (3)
C14—C13—C17—C20	80.2 (2)
C14—C13—C12—C11	56.1 (2)
C14—C13—C12—H12B	177.12
C14—C13—C12—H12A	−64.75
C14—C13—C18—H18A	60.14
C14—C13—C18—H18C	−59.84
C14—C13—C18—H18B	−179.71
C14—C8—C9—C10	−179.7 (2)
C14—C8—C9—C11	−51.6 (2)
C14—C8—C7—C6	−174.7 (2)
C14—C8—C7—H7A	−53.95
C14—C8—C7—H7B	63.95
C14—C15—C16—C17	6.6 (2)
H11A—C11—C12—C13	−176.56
H11A—C11—C12—H12B	62.55
H11A—C11—C12—H12A	−55.70
H11B—C11—C9—C10	59.47
H11B—C11—C12—C13	65.69
H11B—C11—C12—H12B	−55.20
H11B—C11—C12—H12A	−173.45
C10—C9—C8—C7	58.5 (2)
C10—C9—C11—C12	−179.3 (2)
C10—C5—C6—C7	−47.1 (2)
C10—C5—C6—H6A	−168.08
C10—C5—C6—H6B	73.38
C10—C5—C4—C3	−8.00 (19)
C10—C5—C4—H4A	−179.92
C10—C1—C2—C3	−52.5 (2)
C10—C1—C2—H2B	68.47
C10—C1—C2—H2C	−173.32
C7—C8—C14—C13	177.6 (2)
C7—C8—C14—C15	−57.9 (2)
C7—C6—C5—C4	136.9 (4)
H7A—C7—C6—H6A	48.50
H7A—C7—C6—H6B	166.79
H7B—C7—C6—H6A	−69.11
H7B—C7—C6—H6B	49.18
C13—C17—O2—H2	173.56
C13—C17—C16—C15	21.2 (4)
C13—C17—C16—H16A	141.31
C13—C17—C16—H16B	−98.88
C13—C17—C20—H20A	−57.64
C13—C17—C20—H20C	−178.20
C13—C17—C20—H20B	61.83
C13—C14—C15—C16	−32.4 (3)
C13—C14—C15—H15A	−151.46
C13—C14—C15—H15B	86.60
C18—C13—C17—C16	77.3 (2)
C18—C13—C17—C20	−162.2 (2)
C18—C13—C14—C15	−70.1 (2)
C18—C13—C12—H12B	55.00
C18—C13—C12—H12A	173.13
H18A—C18—C13—C17	−49.98
H18A—C18—C13—C12	179.91
H18B—C18—C13—C17	70.17
H18B—C18—C13—C12	−59.94
H18C—C18—C13—C17	−169.96
H18C—C18—C13—C12	59.92
C12—C13—C17—C16	−157.2 (5)
C12—C13—C17—C20	−36.6 (3)
C12—C13—C14—C15	169.2 (2)

C14—C15—C16—H16A	−113.24	H12A—C12—C13—C17	47.93
C14—C15—C16—H16B	126.57	H12B—C12—C13—C17	−70.20
H14A—C14—C13—C17	−66.16	O1—C3—C2—C1	−152.1 (5)
H14A—C14—C13—C12	57.67	O1—C3—C2—H2B	86.61
H14A—C14—C13—C18	178.44	O1—C3—C2—H2C	−30.76
H14A—C14—C8—C7	61.18	O1—C3—C4—H4A	−6.40
H14A—C14—C8—H8A	−178.94	C17—C13—C14—C15	45.3 (3)
H14A—C14—C15—C16	79.03	C17—C16—C15—H15A	125.86
H14A—C14—C15—H15A	−40.05	C17—C16—C15—H15B	−112.84
H14A—C14—C15—H15B	−161.99	C1—C10—O3—H3	72.62
C5—C10—O3—H3	−49.44	C1—C10—C5—C6	171.3 (2)
C5—C10—C9—C8	−54.9 (2)	C1—C10—C5—C4	−12.7 (2)
C5—C10—C9—C11	177.4 (2)	C1—C2—C3—C4	32.0 (3)
C5—C10—C1—C2	42.8 (3)	H1A—C1—C2—C3	−174.53
C5—C10—C1—H1A	164.55	H1A—C1—C2—H2B	−53.58
C5—C10—C1—H1B	−78.56	H1A—C1—C2—H2C	64.62
C5—C6—C7—C8	48.2 (2)	H1B—C1—C2—C3	68.83
C5—C6—C7—H7A	−72.75	H1B—C1—C2—H2B	−170.23
C5—C6—C7—H7B	169.65	H1B—C1—C2—H2C	−52.02
C5—C4—C3—O1	−178.33 (16)	C15—C16—C17—C20	−102.0 (3)
C5—C4—C3—C2	−2.3 (2)	H15A—C15—C16—H16A	6.03
C8—C14—C13—C17	177.3 (2)	H15A—C15—C16—H16B	−114.16
C8—C14—C13—C12	−58.8 (2)	H15B—C15—C16—H16A	127.33
C8—C14—C13—C18	61.9 (2)	H15B—C15—C16—H16B	7.14
C8—C14—C15—C16	−161.9 (2)	C4—C3—C2—H2B	−89.33
C8—C14—C15—H15A	79.02	C4—C3—C2—H2C	153.30
C8—C14—C15—H15B	−42.92	C4—C5—C6—H6A	15.88
C8—C9—C10—C1	−177.8 (2)	C4—C5—C6—H6B	−102.65
C8—C9—C11—C12	53.0 (2)	H4A—C4—C3—C2	169.65
C8—C9—C11—H11A	174.00	H4A—C4—C5—C6	−4.11
C8—C9—C11—H11B	−68.24	C6—C5—C4—C3	167.8 (2)
C8—C7—C6—H6A	169.42	C20—C17—O2—H2	−61.44
C8—C7—C6—H6B	−72.29	C20—C17—C16—H16A	18.10
H8A—C8—C14—C13	−62.51	C20—C17—C16—H16B	137.91
H8A—C8—C14—C15	61.98	H20A—C20—C17—C16	58.97
H8A—C8—C9—C10	−60.73	H20B—C20—C17—C16	178.44
H8A—C8—C9—C11	67.35	H20C—C20—C17—C16	−61.59
H8A—C8—C7—C6	65.34	C16—C17—O2—H2	59.18
H8A—C8—C7—H7A	−173.92		

Hydrogen-bond geometry (Å, º)

D—H···*A*	*D*—H	H···*A*	*D*···*A*	*D*—H···*A*
O2*W*—H4*W*···O2^{i}	0.98	2.05	3.0279 (7)	176
O2*W*—H2*W*···O3^{ii}	0.98	1.82	2.7933 (6)	171
C14—H14*A*···C20	1.10	2.70	3.0951 (7)	101
C11—H11*A*···C1	1.09	2.59	2.9771 (8)	100
C18—H18*A*···C16	1.08	2.63	3.0340 (8)	102

C12—H12*A*···C20	1.09	2.60	3.0209 (8)	102
C2—H2*B*···O2*W*	1.09	2.69	3.5634 (7)	137
O1*W*—H1*W*···O2*W*	0.98	1.85	2.8189 (7)	169
O3—H3···O1*W*	0.98	1.79	2.7672 (6)	172
O1*W*—H3*W*···O2^{iii}	0.98	1.93	2.9053 (6)	172
O2—H2···O1^{iv}	0.98	1.77	2.7352 (6)	168
C6—H6*B*···O1^{v}	1.09	2.56	3.4828 (7)	141

Symmetry codes: (i) *x*−1, *y*+1, *z*; (ii) *x*−1/2, −*y*+3/2, −*z*; (iii) *x*, *y*+1, *z*; (iv) *x*+1, *y*−1, *z*; (v) *x*+1, *y*, *z*.